[Article] Gaussian Specimens for Gigacycle Fatigue Tests: Damping Effects

Available online at www.sciencedirect.com

ScienceDirect

Procedia Engineering 74 (2014) 113 – 118

Procedia Engineering

www.elsevier.com/locate/procedia

XVII International Colloquium on Mechanical Fatigue of Metals (ICMFM17)

Gaussian Specimens for Gigacycle Fatigue Tests: Damping Effects

A. Tridello[a], D.S. Paolino[b], G.Chiandussi[c], M.Rossetto[d]

[a,b,c,d] *Department of Mechanical and Aerospace Engineering, Politecnico di Torino, Turin, Italy*

Abstract

Experimental tests investigating the gigacycle fatigue properties of materials are commonly performed with ultrasonic testing procedures, which allow for a significant reduction of testing time but induce a significant temperature increment in specimens. In order to evaluate the significance of size effects on the fatigue strength of materials, the Authors recently proposed to adopt Gaussian specimens for gigacycle tests. Fatigue specimens were designed without taking into account the hysteretic damping and its effects both on the stress distribution and on the heat power dissipation. However, in order to evaluate the temperature increment and the feasibility of ultrasonic fatigue tests with Gaussian specimens, the total dissipated heat power as well as the distribution of the dissipated heat power density along the specimen must be taken into account.
The present paper proposes an analytical model validated through a finite element analysis, which permits to evaluate the effects of the hysteretic damping on the stress distribution, on the dissipated heat power density distribution and on the total dissipated heat power in Gaussian specimens.

Selection and peer-review under responsibility of the Politecnico di Milano, Dipartimento di Meccanica

Keywords: gigacycle fatigue; very-high-cycle fatigue; risk-volume; ultrasonic testing machine; power dissipated.

1. Introduction

In recent years, very-high-cycle fatigue (VHCF) behavior of metallic materials has become a major point of interest for researchers and industries. The needs of specific industrial fields (aerospace, mechanical and energy industry) for structural components with increasingly large fatigue lives, up to 10^{10} cycles (gigacycle fatigue), requested for a more detailed investigation on the experimental properties of materials in the VHCF regime.

Gigacycle fatigue tests are commonly performed using resonance fatigue testing machines [1,2] with a loading frequency of 20 kHz (ultrasonic tests). Experimental results have shown that failure is due to cracks which nucleate at the specimen surface if the stress amplitude is above the conventional fatigue limit (surface nucleation) and that failure is generally due to cracks which nucleate from inclusions or internal defects (internal nucleation) when specimens are subjected to stress amplitudes below the conventional fatigue limit [3]. Following the experimental evidence, new phenomenological models for the description of fatigue life were also introduced [4]: models that can

Selection and peer-review under responsibility of the Politecnico di Milano, Dipartimento di Meccanica
doi:10.1016/j.proeng.2014.06.234

take into account the occurrence of two different failure modes (Duplex S-N curves) have integrated classical fatigue life models, characterized by failures due to a single failure mode and by the presence of the fatigue limit.

Together with the introduction of new fatigue life models, the research on VHCF focused also on the study of the factors affecting the gigacycle fatigue properties of materials. In particular, size effects have recently gained significant attention [5]. In [6], the Authors proposed a specimen shape (Gaussian specimen), characterized by a large region of material subjected to a uniform stress distribution (risk-volume). The Gaussian specimen was designed without taking into account the hysteretic damping and its effect on heat power dissipation. However, the large risk-volume of Gaussian specimens requires a sound evaluation of the effects due to the hysteretic damping both on the stress distribution and on the heat power dissipation.

The present paper proposes an analytical model for the prediction of the stress distribution and of the heat power dissipation, in case of Gaussian specimens with hysteretic damping. The Gaussian profile is approximated with a cosine function and the analytical models of the stress distribution, the (average) heat power density and the (average) total dissipated heat power are determined. Finally, the analytical models are validated numerically through a Finite Element Analysis.

Nomenclature

$A_1, A_2, A_3, A_4\ A_5$	constant coefficients
α_2, α_3	geometrical parameters of the specimen
D_1, D_2, D_3	characteristic diameters of the specimen
$D(\cdot)$	diameter function in specimen part 3
E_d	complex elastic modulus
E_r	real part of the complex elastic modulus
$\varepsilon_i(\cdot)$	strain amplitude in the i-th specimen part
f_0	resonance frequency of the specimen
η	loss factor
$L_1, L_2, L_3, L_4, L_5, L$	characteristic lengths of the specimen
P_{diss}	(average) total heat power dissipated
P_{in}	(average) mechanical/electrical power supplied
$\dot{q}_i(\cdot)$	(average) heat power density dissipated in the i-th specimen part
$S_i(\cdot)$	cross-section of the i-th specimen part
T	load period
$u_i(\cdot)$	displacement amplitude in the i-th specimen part
$\sigma_i(\cdot)$	stress amplitude in the i-th specimen part
z	longitudinal coordinate of the specimen
z_i	longitudinal coordinate in the i-th specimen part

2. Analytical design

Internal dissipation in Gaussian specimens is modeled by considering a hysteretic damping model. The complex elastic modulus E_d ($E_d = E_r(1 + \mathbb{i}\,\eta)$) is introduced in order to take into account the hysteretic damping: the real part of the elastic modulus, E_r, takes into account the elastic energy stored by the vibrating body, while the imaginary part ηE_r, being η the loss factor, takes into account the amount of energy dissipated due to internal friction. In presence of hysteretic damping, a closed-form solution for the stress distribution in the Gaussian specimen part cannot be determined. Therefore, the Gaussian profile is approximated with a cosine function (Section 2.1) and the stress distribution along the specimen length is determined (Section 2.2). Finally, the (average) heat power density dissipated along the longitudinal axis and the (average) total dissipated heat power are analytically determined from the computed stress distribution (Section 2.3).

2.1. Approximation of the Gaussian profile

Figure 1 shows the typical shape of a Gaussian specimen [6].

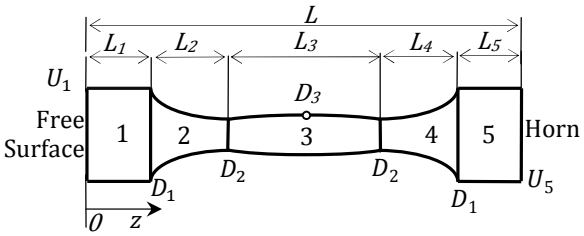

Fig. 1. Typical Gaussian specimen.

In order to determine the displacement and the stress amplitude in specimen part 3, the Gaussian profile is approximated by a cosine function. The expression of the cross-section diameter, $D(z)$, of the approximating cosine function can be obtained by imposing the passage of the cosine function through the points $(L_1 + L_2; D_2)$ and $(L/2\,; D_3)$ defined in Fig. 1. The approximating cosine function is expressed by:

$$D(z) = D_3 \cos\left[\alpha_3 \left(z - \frac{L}{2}\right)\right], \tag{1}$$

where $\alpha_3 = 2\,\mathrm{acos}\left[\frac{D_2}{D_3}\right]/L_3$. In case of L_3 larger than 50 mm, the cosine approximation entails a maximum percent error smaller than 1%.

2.2. Stress distribution

The displacement amplitude in each specimen part ($i = 1, \ldots, 5$ in Fig. 1) can be expressed by Equation 2:

$$\begin{cases} u_1(z_1) = A_1 \cos(kz_1) + B_1 \sin(kz_1), & 0 \le z_1 \le L_1 \\ u_2(z_2) = \dfrac{A_2 \cos\left(z_2\sqrt{k^2-\alpha_2^2}\right) + B_2 \sin\left(z_2\sqrt{k^2-\alpha_2^2}\right)}{\cosh[\alpha_2(z_2-L_2)]}, & 0 \le z_2 \le L_2 \\ u_3(z_3) = \dfrac{A_3 \cos\left(z_3\sqrt{k^2+\alpha_3^2}\right) + B_3 \sin\left(z_3\sqrt{k^2+\alpha_3^2}\right)}{\cos[\alpha_3(z_3-L_3)]}, & 0 \le z_3 \le L_3 \\ u_4(z_4) = \dfrac{A_4 \cos\left(z_4\sqrt{k^2-\alpha_2^2}\right) + B_4 \sin\left(z_4\sqrt{k^2-\alpha_2^2}\right)}{\cosh[\alpha_2 z_4]}, & 0 \le z_4 \le L_4 \\ u_5(z_5) = A_5 \cos(kz_5) + B_5 \sin(kz_5), & 0 \le z_5 \le L_5 \end{cases}, \tag{2}$$

where $u_i(\cdot)$ denotes the displacement amplitude in each specimen part ($i = 1 \ldots 5$), N is the ratio D_1/D_2, $\alpha_2 = \mathrm{acosh}(N)/L_2$, and A_1, A_2, A_3, A_4 and A_5 are complex coefficients, which can be determined by imposing proper boundary conditions.

At the specimen free surface ($z = 0$), the real part of the displacement amplitude is equal to U_1 (Fig. 1), while the imaginary part of displacement amplitude, the real and the imaginary parts of the strain amplitude are equal to 0:

$$\begin{cases} \mathrm{Re}[u_1(z_1 = 0)] = U_1 \\ \mathrm{Im}[u_1(z_1 = 0)] = 0 \\ \mathrm{Re}[\varepsilon_1(z_1 = 0)] = 0 \\ \mathrm{Im}[\varepsilon_1(z_1 = 0)] = 0 \end{cases}, \tag{3}$$

where $\varepsilon_i(\cdot)$ denotes the strain amplitude in each specimen part ($i = 1 \dots 5$). The other constant coefficients are determined by imposing the continuity of the real and imaginary part of displacement amplitude and strain amplitude at the interface between two adjacent specimen parts:

$$\begin{cases} \mathrm{Re}\left[u_j\left(z_j = L_j\right)\right] = \mathrm{Re}\left[u_{j+1}\left(z_{j+1} = 0\right)\right] \\ \mathrm{Im}\left[u_j\left(z_j = L_j\right)\right] = \mathrm{Im}\left[u_{j+1}\left(z_{j+1} = 0\right)\right] \\ \mathrm{Re}\left[\varepsilon_j\left(z_j = L_j\right)\right] = \mathrm{Re}\left[\varepsilon_{j+1}\left(z_{j+1} = 0\right)\right] \\ \mathrm{Im}\left[\varepsilon_j\left(z_j = L_j\right)\right] = \mathrm{Im}\left[\varepsilon_{j+1}\left(z_{j+1} = 0\right)\right] \end{cases}, \tag{4}$$

for $j = 1, \dots, 4$ (it is worth noting that, due to the symmetry, L_4 is equal to L_2 and L_5 is equal to L_1). The stress distribution in each specimen part is $\sigma_i(z_i) = E_d \varepsilon_i(z_i)$ ($i = 1, \dots, 5$).

2.3. Dissipated heat power

Due to hysteretic damping, heat power is dissipated in the Gaussian specimen. Equation 5 expresses the (average) heat power density dissipated [7] in each specimen part ($i = 1, \dots, 5$):

$$\dot{q}_\iota(z_i) = \frac{1}{T}\int_0^T \mathrm{Re}[\sigma_i(z_i, t)]\mathrm{Re}\left[\frac{\partial \varepsilon_i(z_i,t)}{\partial t}\right] dt, \tag{5}$$

where T is the load period. By assuming the linear elasticity of the material, Equation 5 can be rewritten as:

$$\dot{q}_\iota(z_i) = E_r \pi \eta f_0 |\varepsilon_i(z_i)|^2, \tag{6}$$

where f_0 is the resonance frequency of the specimen and $|\varepsilon_i(z_i)|$ is the Euclidean norm of the strain amplitude (i.e., $|\varepsilon_i(z_i)| = \sqrt{\mathrm{Re}[\varepsilon_i(z_i)]^2 + \mathrm{Im}[\varepsilon_i(z_i)]^2}$). The (average) total heat power dissipated in a load cycle is the sum of the (average) heat power density dissipated in each specimen part (Equation 6) integrated with respect to the volume of the corresponding specimen part:

$$P_{diss} = \sum_{i=1}^{5} \int_0^{L_i} \dot{q}_\iota(z_i)\, S_i(z_i) dz_i, \tag{7}$$

where $S_i(z_i)$ denotes the cross-section of the i-th specimen part. The (average) mechanical/electrical power supplied by the ultrasonic generator during one cycle can be expressed as:

$$P_{in} = \frac{1}{T}\int_0^T S_5(L_5)\mathrm{Re}[\sigma_5(L_5, t)]\mathrm{Re}\left[\frac{\partial \varepsilon_5(L_5,t)}{\partial t}\right] dt \tag{8}$$

It is worth noting that the (average) total dissipated heat power must be equal to the (average) mechanical/electrical power supplied by the ultrasonic generator during one cycle (i.e., $P_{diss} = P_{in}$).

3. Finite Element Validation

The (average) heat power density along specimen length and the (average) total dissipated heat power at the first longitudinal frequency are evaluated through Finite Element Analyses (FEA) in four Gaussian specimens with different risk-volumes (volume of material subjected to an applied stress amplitude above the 90% of the applied maximum stress amplitude [4]). The characteristics of each specimen are reported in Table 1:

Table 1. Characteristics of specimens used for FEA.

	D_2 [mm]	L_3 [mm]	Risk-volume [mm^3]
Specimen 1	8	10	1200
Specimen 2	10	10	1974
Specimen 3	8	27.5	3124
Specimen 4	10	27.5	5118

The numerical analyses are carried out by using the commercial finite element program ANSYS. Eight-node quadrilateral elements (plane 82) with the axisymmetric option are used for the finite element models. The numerical models count for a number of elements ranging from 12000 to 25000 elements. The Gaussian specimens considered for the analysis have been designed considering steel (E_r equal to 211 GPa, Poisson's ratio equal to 0.29, material density equal to 7800 kg/m^3 and loss factor η equal to 0.00047 [8]). The specimens are loaded by imposing a harmonic nodal displacement at the interface between specimen and horn ($z = L$). The harmonic displacement is determined by considering the analytical amplification factor [6] in order to have a stress amplitude equal to 500 MPa in the Gaussian specimen part.

For each Gaussian specimen, Fig. 2 reports the (average) heat power density dissipated with respect the non-dimensional coordinate (z/L). Plotted values are computed by using the longitudinal stress distribution obtained with the analytical model and the longitudinal stress distribution along the longitudinal axis obtained with FEA.

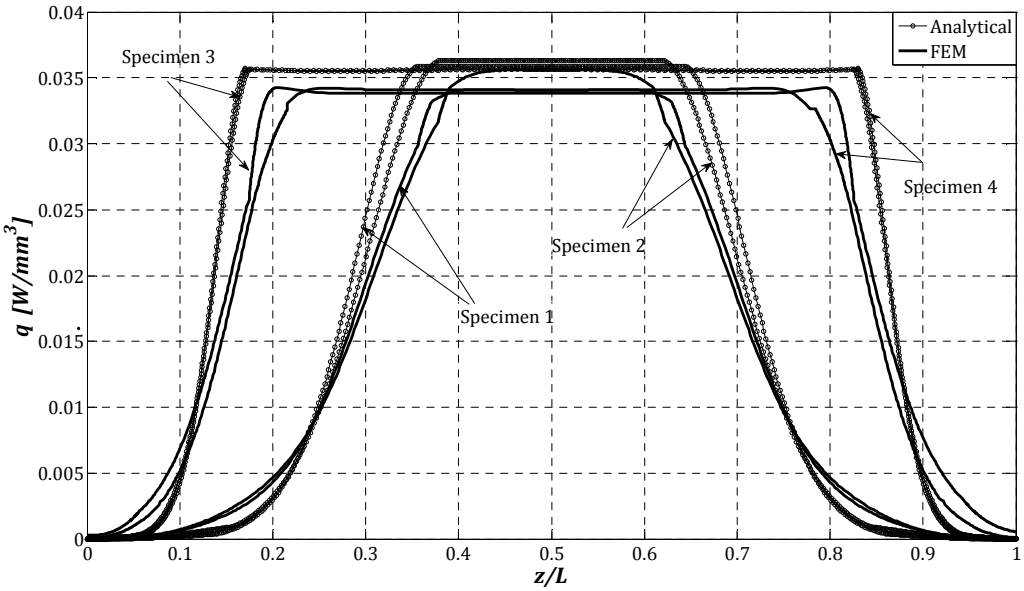

Fig. 2. Average dissipated heat power density along the longitudinal axis.

According to Fig. 2, the (average) dissipated heat power densities computed by using the analytical model and the numerical model have similar qualitative trends. However, the FEA model gives smaller maximum densities: for the same applied harmonic displacement, the stress in the Gaussian specimen part computed through FEA is about 1.5% smaller than the stress computed through the analytical model. As a consequence, considering Equation 5, the (average) dissipated heat power density computed through FEA is smaller. The difference increases as the Gaussian specimen length increases: however, for the analyzed cases, the maximum difference is smaller than 0.01 W/mm^3.

Finally, the (average) total heat dissipated power is evaluated by using the analytical model (Equation 7) and through FEA. Considering FEA, the (average) total dissipated heat power is evaluated as the sum of the (average)

heat power density dissipated (Equation 6) in each element multiplied by the volume of the corresponding element. Both normal strains and shear strains are considered for the computation from FEA.

Table 2 reports the (average) total dissipated heat power evaluated by considering the analytical model and FEA together with the percent difference.

Table 2. Total dissipated power obtained through the analytical model and through FEA.

	Analytical Model [W]	FEA [W]	Percent difference
Specimen 1	65	72	10%
Specimen 2	105	119	11%
Specimen 3	131	144	9%
Specimen 4	211	238	11%

According to Table 2, the (average) total dissipated heat power is larger if computed through FEA. In the computation of the total heat power with FEA, the contribution of each stress component is taken into account, while, in the analytical model, only the longitudinal normal stress is considered for the power computation. For the considered cases, the percent difference between the results obtained by using the two approaches is limited and ranges from 9% to 11%. The Gaussian specimen with the largest risk-volume has the largest (average) total dissipated heat power. It must be noted that the largest (average) total dissipated heat power is significantly smaller than the maximum mechanical/electrical power which can be supplied by ultrasonic generators commonly used for gigacycle fatigue tests (between 2 kW and 4 kW).

4. Conclusions

An analytical model for the evaluation of stress distribution, of the (average) dissipated heat power density and of the (average) total dissipated heat power in Gaussian specimens has been proposed in the paper. The analytical model has been validated through FEA. Considering the (average) total dissipated heat power, the difference between the two approaches is in general limited (about 10%). If the Gaussian specimen with the largest risk-volume (5118 mm^3) is taken into account, the total dissipated heat power is smaller than 215 W and is thus significantly smaller than the maximum mechanical/electrical power that can be supplied by ultrasonic generators commonly adopted for gigacycle fatigue tests.

Acknowledgements

The authors gratefully acknowledge financial support from the Piedmont Region Industrial Research Project NGP - Bando Misura II.3.

References

[1] C. Bathias, P.C. Paris, Gigacycle fatigue in mechanical practice. CRC Dekker, New York, 2005.
[2] S. Stanzl-Tschegg, Very high cycle fatigue measuring techniques, Int. J. Fatigue 60 (2014) 2-17.
[3] H. Mughrabi, On 'multi-stage' fatigue life diagrams and the relevant life-controlling mechanisms in ultrahigh-cycle fatigue, Fatigue Fract. Eng. Mater. Struct. 25 (2002) 755-764.
[4] D.S Paolino, G. Chiandussi, M. Rossetto, A unified statistical model for S-N fatigue curves: probabilistic definition, Fatigue Fract. Eng. Mater. Struct. 36 (2013), 187-201.
[5] Y. Furuya, Specimen size effects on gigacycle fatigue properties of high-strength steel under ultrasonic fatigue testing, Scripta Mater. 58 (2008) 1014–1017.
[6] D.S. Paolino, A. Tridello, G. Chiandussi, M. Rossetto, On specimen design for size effect evaluation in ultrasonic gigacycle fatigue testing, Fatigue Fract. Eng. Mater. Struct (In press), doi: 10.1111/ffe.12149
[7] A.D. Nashif, D.I.G. Jones, J.P. Henderson, Vibration damping, first ed., Wiley, New York, (1985).
[8] M.F. Ashby, Materials selection in mechanical design, forth ed., Butterwoth-Heinemann, Oxford, (2010).